Conference Paper, Published Version

Farahani, Rozita J.; Dalrymple, Robert A.; Hérault, Alexis; Bilotta, Giuseppe; Rustico, Eugenio

Modeling the Coherent Vortices in Breaking Waves

Modeling the coherent vortices in breaking waves

Rozita Jalali Farahani
Department of Civil Engineering
Johns Hopkins University
Baltimore, MD 21218, USA
rozita@jhu.edu

Robert A. Dalrymple
Department of Civil Engineering
Johns Hopkins University
Baltimore, MD 21218, USA
rad@jhu.edu

Alexis Hérault
Conservatoire National des Arts et Métiers
Paris, France
Istituto Nazionale di Geofisica e Vulcanologia Italy
Catania, Italy

Giuseppe Bilotta
Istituto Nazionale di Geofisica e Vulcanologia Italy
Catania, Italy

Eugenio Rustico
Bundesanstalt Für Wasserbau
Karlsruhe, Germany

***Abstract*—Breaking water waves at the shoreline create a wide range of turbulent structures in the water column. Plunging waves are particularly interesting as the plunging tip of the wave impacts into the toe of the wave, often creating a tube or barrel of air that surfers enjoy. As a result, the turbulence left after the passage of the wave consists, in part, of coherent horseshoe (hairpin) vortices that sink deeper into the water column with time. Nadaoka et al. (1989) identified the legs of the horseshoe (hairpin) vortices as obliquely descending eddies; here we show they are just part of the horseshoes (hairpins). We also provide an argument for the creation of these hairpin vortices (Farahani et al., 2014b), based on an analogy with turbulent boundary layers.**

I. Introduction

Water wave breaking at the shoreline produces turbulence, which can play an important role in the sediment transport, wave damping, and safety of vessels and structures located in the surf zone (Banner and Peregrine, 1993). Not only do waves periodically breaking on a beach give rise to these coherent vortical structures, but a solitary wave does as well. One of the important differences with a solitary wave (which is a first order approximation of a tsunami) is that here there is no pre-existing turbulence in the water column prior to the arrival of the wave as is the case for waves on beaches. Therefore, we can study three-dimensional vortex structures separately from the effect of returning undertow and the residual turbulence induced from the previously broken waves in the case of periodic waves.

Breaking water waves including solitary waves have been previously modeled using Smoothed Particle Hydrodynamics (SPH) method by several researchers such as Monaghan and Kos (1999); Monaghan and Kos (2000); Dalrymple et al. (2002); Colagrossi and Landrini (2003); and Dalrymple and Rogers (2006). In this study, we use three-dimensional Smoothed SPH method to model broken solitary waves as well as to investigate the induced three-dimensional vortex structures and turbulent fields. Two different solitary wave types (spilling wave and plunging wave) are studied and coherent vortex structures associated with each type are investigated. Our computations are carried out with the GPUSPH model (Hérault et al. 2010), which uses massively parallel Nvidia graphics cards.

II. Governing equations and GPUSPH model

The governing equations to model the water wave motion consist of the conservation of mass and the conservation of momentum as:

$$\frac{\partial \rho}{\partial t} + \rho(\nabla . \vec{u}) = 0 \tag{1}$$

$$\frac{D\vec{v}}{Dt} = -\frac{1}{\rho}\nabla P + \vec{g} + \vec{\Theta} \tag{2}$$

where ρ is density; t is time; $\vec{u}$ is velocity; P is the pressure; $\vec{g}$ is the gravitational acceleration; and $\vec{\Theta}$ is the viscous term. The conservation of mass equation can be written in SPH form as:

$$\frac{\partial \rho_a}{\partial t} = \sum_b m_b(\vec{u}_a - \vec{u}_b)\nabla_a W(r_{ab}) \tag{3}$$

where a denotes the particle of interest; b denotes the neighboring particle; m is the particle mass; W is the kernel function; and r_{ab} is the distance between particle a and particle b.

The first term of the right hand side of the momentum equation (2) is the pressure gradient term that can be written in the SPH form as:

$$-\sum_b (\frac{P_a}{\rho_a^2} + \frac{P_b}{\rho_b^2}) m_b \nabla_a W(r_{ab}) \tag{4}$$

The second term on the right hand side of the momentum equation is the gravitational acceleration, which is defined as: $\vec{g} = (0, 0, 9.81)\frac{m}{s^2}$. The third term on the right hand side of the momentum equation is the viscous term that can be computed using several methods. In this study we have used the SPS approach of Dalrymple and Rogers (2006) with constant Smagorinsky coefficient. In the SPS approach, the effect of turbulence is considered in the SPH method using a model similar to the Sub-Grid Scale (SGS) turbulence model in the Large Eddy Simulation (LES) method (Dalrymple and Rogers, 2006).

GPUSPH model is an open source package ($http://www.ce.jhu.edu/dalrymple/GPUSPH/Home.html$) that was introduced by Hérault et al. (2010). GPUSPH model performs real-time parallel SPH computations on Graphics Processing Units (GPUs) of computers. GPUSPH is written in an object-oriented platform and consists of several interacting objects. In an Object-Oriented Program (OOP), a set of objects interacts with each other, as opposed to the non-OOP models, in which a program consists of a set of subroutines each performing a particular task. Therefore, the object-oriented programs are easier to maintain, modify, and expand. A couple of additional features are added to the existing package to perform wave-related numerical modeling (Farahani et al., 2014a). These features include finding fluid parameters at Eulerian nodes as well as Lagrangian particles, which leads to a better comparison between numerical SPH results and Eulerian experimental results. The second feature is a procedure for the detection of the particles that form the free surface. GPUSPH is written in the Compute Unified Device Architecture (CUDA) language that is designed for general-purpose computations on Nvidia GPUs. The CUDA language is an extension to the standard programming languages such as C, C++, and FORTRAN (www.nvidia.com).

III. SPH MODELING OF BROKEN SOLITARY WAVES AND THE THREE-DIMENSIONAL HORSESHOE VORTEX STRUCTURES

Coherent vortex structures have been studied in the laboratory by Nadaoka et al. (1989). Two-dimensional spanwise vortex structures were found under breaking waves with axes parallel to the crest line. Behind the wave crest, three-dimensional structures were observed that were called *obliquely descending eddies*. These experiments revealed that the vortex structures induced by breaking waves carry large amounts of vorticity into otherwise almost irrotational velocity fields. Ting and Kirby (1994, 1995, 1996) carried out a series of experiments regarding the plunging and spilling breakers and related turbulence . The experiments revealed that the vortex structures carry turbulent kinetic energy. In the case of a plunging breaker, they reported that the kinetic energy is transported landward and dissipated within one wave cycle. In the case of a spilling breaker, the turbulent kinetic energy is transported seaward and the dissipation rate is much slower.

An experimental study of a broken solitary wave and corresponding turbulence was performed by Ting (2006). In this study, another type of coherent structures, called downbursts, were detected as well as the obliquely descending eddies.

In terms of numerical studies, Lin and Liu (1998) carried out a two dimensional RANS numerical model to study the wave breaking in the surf zone. They reported that the turbulence generation is started from a 'roller' region in front of the broken wave. Watanabe et al. (1999) used a three-dimensional large-eddy simulation (LES) method to study the turbulent vortices under spilling and plunging breakers. Christensen and Deigaard (2001) and Christensen (2006) performed a LES method to model spilling and plunging breakers. They found the same order of magnitude of the turbulent energy as the previous experimental results.

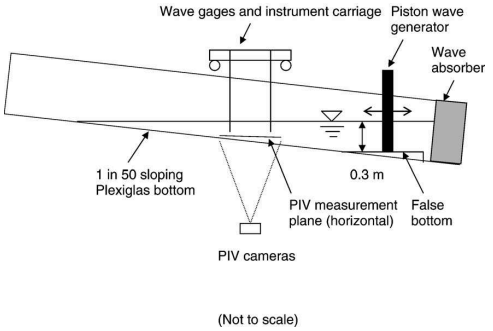

Fig. 1. Schematic plot of experimental set-up (Ting, 2006)

SPH method has been previously proven to be capable of modeling broken water waves. In this section, we show that SPH method is also capable of capturing the turbulence induced from the broken waves and the corresponding coherent vortices. For this purpose, the laboratory-scale solitary breaking wave of Ting (2006) is chosen to be numerically modeled by the SPH method.

A. Wave tank set-up

The wave tank set-up used in the numerical model was inspired by the experimental study of Ting (2006). The wave tank is 25 m long, 0.9 m wide and the bottom plane has a slope of 1 in 50. The still water depth is equal to 0.3 m and a piston type wave generator produces a spilling solitary wave with a wave height of 0.22 m. Figure 1 illustrates a schematic plot of the experimental set-up (Ting, 2006).

B. SPH modeling of the solitary wave

GPUSPH model is used to carry out the numerical simulation with initial particle spacing of particles equal to 0.007 m and about seven million particles are used in this simulation. The Wendland kernel function (1995) is used for the SPH interpolation. A zeroth-order Shepard filter (Shepard, 1968) is implemented to reinitialized the density once every 30 time steps.

The piston wave generator is presented as a moving boundary in the numerical model and the solitary wave is generated using the Goring and Raichlen (1980) approach. The solitary wave is generated using the following equation (Goring and Raichlen, 1980):

$$\frac{\zeta(t)}{S} = \frac{1}{2}\{1+\tanh 2[(3.8+\frac{H}{h})(\frac{t}{\tau}-\frac{1}{2})-\frac{H}{h}(\frac{\zeta}{S}-\frac{1}{2})]\} \quad (5)$$

where ζ is the wave generator displacement; S is the stroke; H is the wave height; h is the water depth; t is time; and τ is duration of wave generator motion.The solitary wave generation trajectory in our problem is computed using equation 5 and presented in the figure 2. Here, the wave height is equal to 0.22 m and the water depth is equal to 0.3 m.

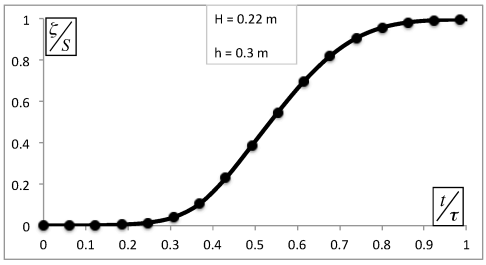

Fig. 2. Solitary wave piston trajectory

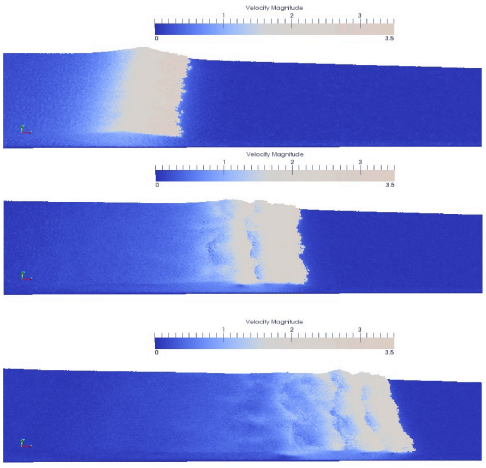

Fig. 3. Numerical results of solitary wave breaking as a spilling breaker at time = 3, 3.5, 4s

The solitary wave breaks as a spilling breaker, hits the water surface ahead and splashes up. Then a sequence of overturning and splashing up occurs as presented in figure 3.

C. Generation and evolution of three-dimensional coherent structures

A coherent turbulent structure can be defined as "A connected turbulent fluid mass with instantaneously phase-correlated vorticity over its spatial extent" (Hussain, 1986). In the past decades several studied have been conducted on the coherent structures since they present organized structures in a turbulent field with random, three-dimensional vorticity. Therefore, studying the configuration of these organized structures helps us have a better understanding of turbulent motions. Coherent structures can be evolved in various physical configurations such as roller, rib, horseshoe (hairpin), toroidal, helical, bihelical, etc. These structures play an important role in the transport of mass, momentum, and heat and hence a number of various coherent detection schemes have been developed to capture them. In this study, we used λ_2, which has been widely used in the previous studies to detect the vortex cores.

Jeong and Hussain (1994) first introduced the λ_2 criterion, which is used to identify the coherent structures. In this method, the tensor $S^2 + \Omega^2$ is calculated where S and Ω are the symmetric and antisymmetric components of velocity gradient tensor $\nabla\vec{u}$. The term λ_2 is identified as the second largest eigenvalue of this tensor and a vortex core is defined as a region with a negative λ_2 threshold. The size of the coherent structures varies using different λ_2 thresholds but the core geometry of the coherent structure is not sensitive to the value of λ_2. Figure 4 illustrates the coherent structures under the broken solitary wave, identified by the isosurface of $\lambda_2 = -50$.

This picture shows the time history of generation and evolution of coherent structures that are mostly in the form of reversed horseshoe structures. In this picture the flow field is observed from above in a wave-following frame of reference. The phrase "reversed" is used because the configuration of these coherent structures are reversed in comparison to the horseshoe structures observed in a boundary layer problem (Green, 1995). Figure 5 illustrates a schematic comparison of horseshoe structures under a broken water wave and in a boundary layer problem. In a boundary layer problem, the vertical velocity gradient initiates horseshoe structures from the spanwise rollers at the locations of higher curvature. In a wave breaking problem, in a wave-following frame of reference, the same mechanism happens but in the reversed direction of the flow motion. Therefore, the rotations of the legs are still counter-rotation in a wave breaking problem but in the reversed direction of the ones in a boundary layer problem.

When a wave breaks, two-dimensional spanwise rollers are generated under the broken wave at the locations of overturning. Later, three-dimensional reversed horseshoe structures are initiated from the locations of the spanwise rollers that have higher curvature.The generated reversed horseshoe structures are denoted by letter in picture 4 as A,B,...,P. At time = 3.5 s, when the solitary wave is already broken, three reversed horseshoe structures (A,B, and C) start to evolve. At time = 3.7 s, another two reversed horseshoe structures (D, E) are generated from the second overturning location (splash-up). As time passes by, these structures evolve and propagate in -x-direction (from right to left) in the wave-following frame of reference. They also go downward to deeper layers of the water column. Some of the reversed horseshoe structures tear up (vortex structure A, tears up at time = 4.1 s). New horseshoe structures are generated at time = 4.5 s (F, G, H), time = 4.9 s (I, L), time = 5.1 (J,K), time = 5.3 s (M,N), and time = 5.5 s (O,P).

D. Turbulent kinetic energy and momentum flux associated with the coherent structures

The instantaneous velocity is decomposed to ensemble averaged velocity and the turbulent velocity as:

$$\vec{u} = < \vec{u} > + \vec{u}' \tag{6}$$

where $< \vec{u} >$ is the ensemble averaged velocity and $\vec{u}'$ is the turbulent velocity. Therefore, turbulent velocities can be found by subtracting the ensemble averaged velocities from the instantaneous velocities. Turbulent kinetic energy can be found as:

$$k = (u'^2 + v'^2 + w'^2)/2 \tag{7}$$

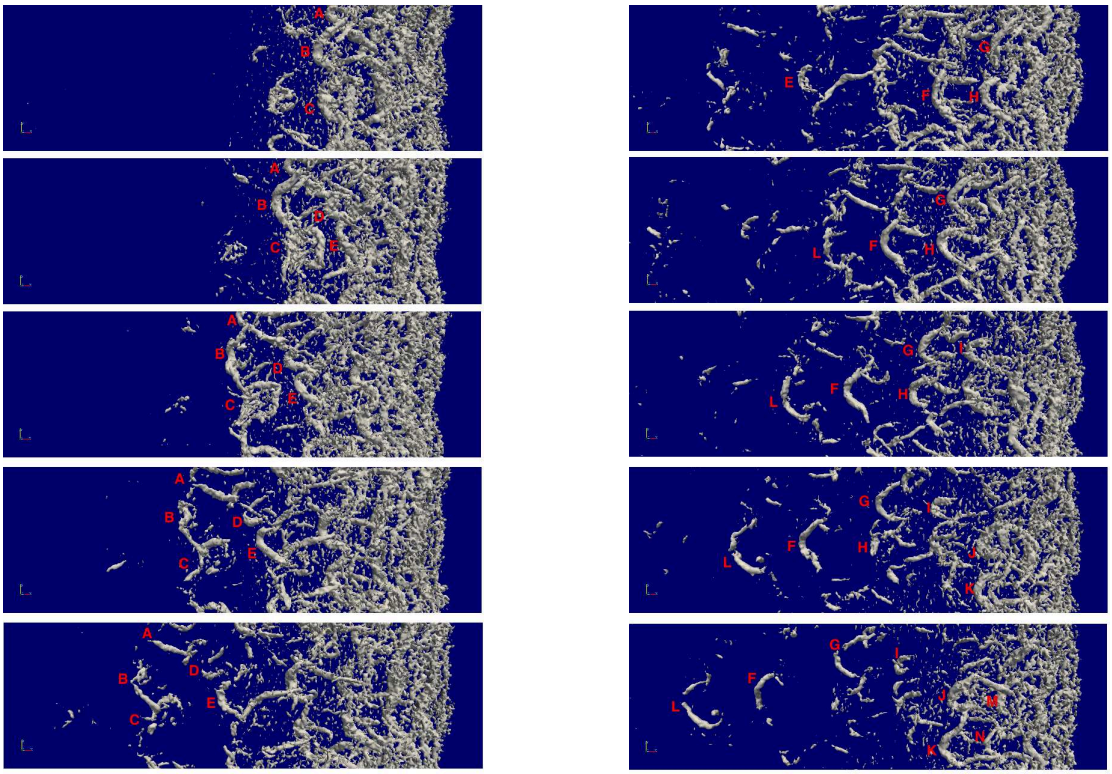

(a) Time = 3.5s, 3.7s, 3.9s, 4.1s, 4.3s, (b) Time = 4.5s, 4.7s, 4.9s, 5.1s, 5.3s.

Fig. 4. Vortex evolution after the broken wave. The flow field is observed from above in a *wave-following* frame of reference at different times (top to bottom in each column).The vortex structures are detected by the isosurface of $\lambda_2 = -50$.

where u', v', w' are turbulence velocity components in x,y, and z direction. The six components of turbulence stresses are found as: u'^2, v'^2, w'^2, $u'v'$, $u'w'$,$v'w'$.

Figure 6 presents the vortex structures behind the broken wave at time = 4.7 s. This picture also presents streamwise vorticity profile (ω_x), turbulent velocity vectors (v', w'), turbulent momentum flux ($-u'w'$), and turbulent kinetic energy. Turbulent velocity vectors and streamwise vorticity show two counter-rotating rotations associated with the two legs of a reversed horseshoe structure. A high value of turbulent momentum flux and turbulent kinetic energy are observed at the location of the reversed horseshoe structure.

The reversed horseshoe structures shown in figure 6 is chased over time and is presented in figure 7. This figure shows the variation of turbulent velocities vectors (v', 'w') and the turbulent momentum flux ($-u'w'$) over time. As the time passes, the reversed horseshoe structure illustrates a downwelling motion and transfer turbulent momentum flux to deeper layers of the water column. The results are consistent with Kim and Moin (1986) and Yang and Shen(2009) results who have also studied the coherent structures but in other problems. As the horseshoe travels downward, the intensity of the turbulent momentum flux decreases due to the spreading and dissipation.

E. Vortex structures under a broken plunging solitary wave

In the previous sections, vortex structures under a spilling water wave have been studied. In this section a plunging solitary wave and the corresponding vortex structures will be studied. Different types of waves can be categorized as follows:

$$\zeta_0 = \frac{tan\beta}{\sqrt{\frac{H_0}{L_0}}} \tag{8}$$

where β is the beach slope, H_0 is the wave height, L_0 is the wave length, and ζ_0 is a criterion to show the breaker type. A wave is a spilling breaker if $\zeta_0 < 0.5$, a plunging breaker if $0.5 < \zeta_0 < 3.3$, and a surging beaker if $\zeta_0 > 3.3$. In the previous sections, in case of the spilling breaker ζ_0 was equal to 0.099. In the following section a plunging wave with the ζ_0 equal to 0.55 will be numerically modeled.

The same wave tank set-up is used only the beach slope is changed from 1 in 50 to 1 in 9. The wave height is equal to 0.22 m and the water depth close to the wave generator is equal to 0.3 m. Figure 8 shows the plunging solitary wave breaking at the beach and the corresponding run-up. The vortex structures are generated under the broken wave and are carried towards the shore by the run-up but no reversed horseshoe structure is observed at the back of the broken wave

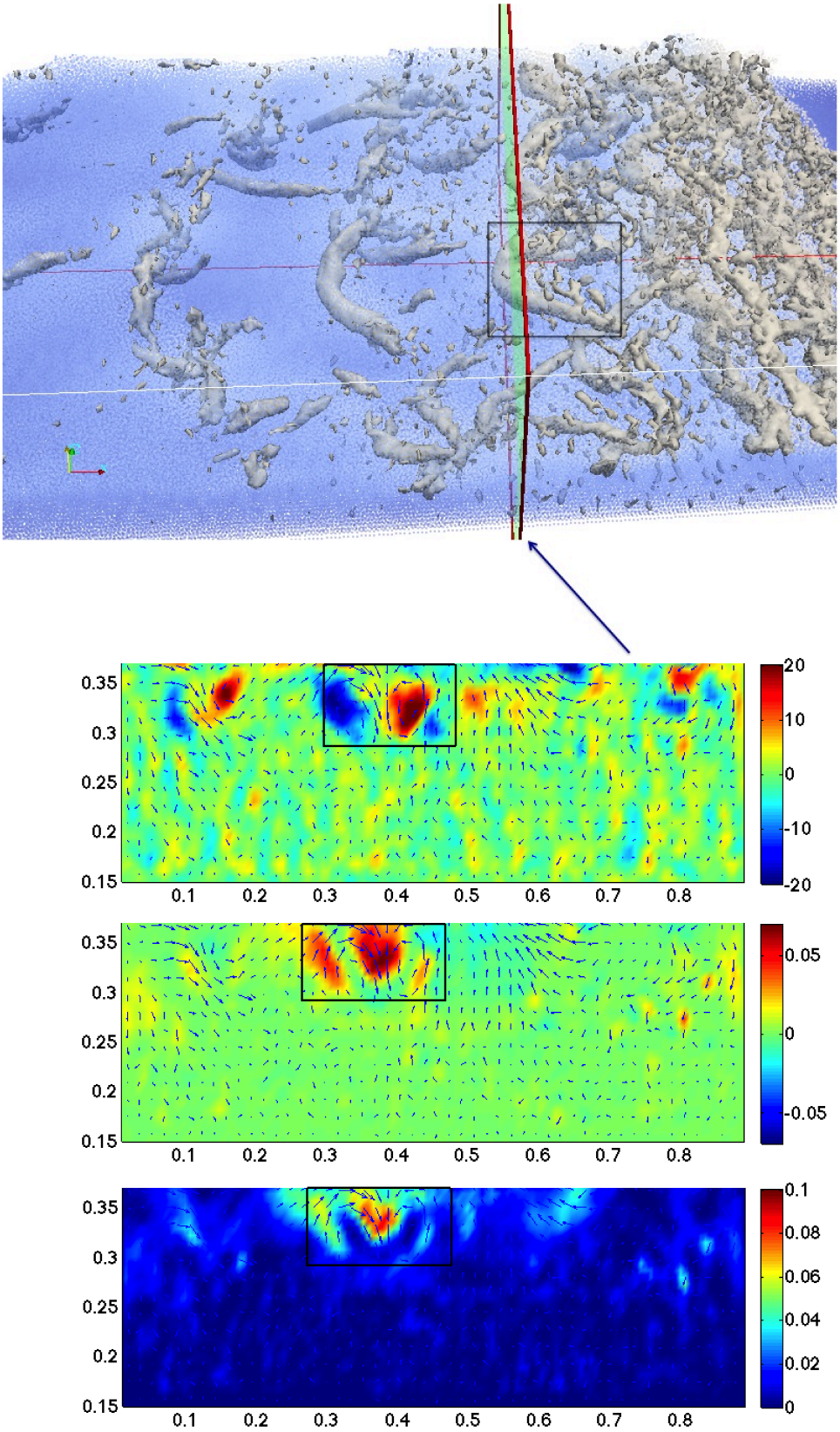

Fig. 6. Reversed horseshoe structures at time = 4.7 s. From top to bottom: (a) Streamwise vorticity profile (ω_x) and turbulent velocity vectors (v', w'), (b) turbulent momentum flux ($-u'w'$), (c) Turbulent kinetic energy

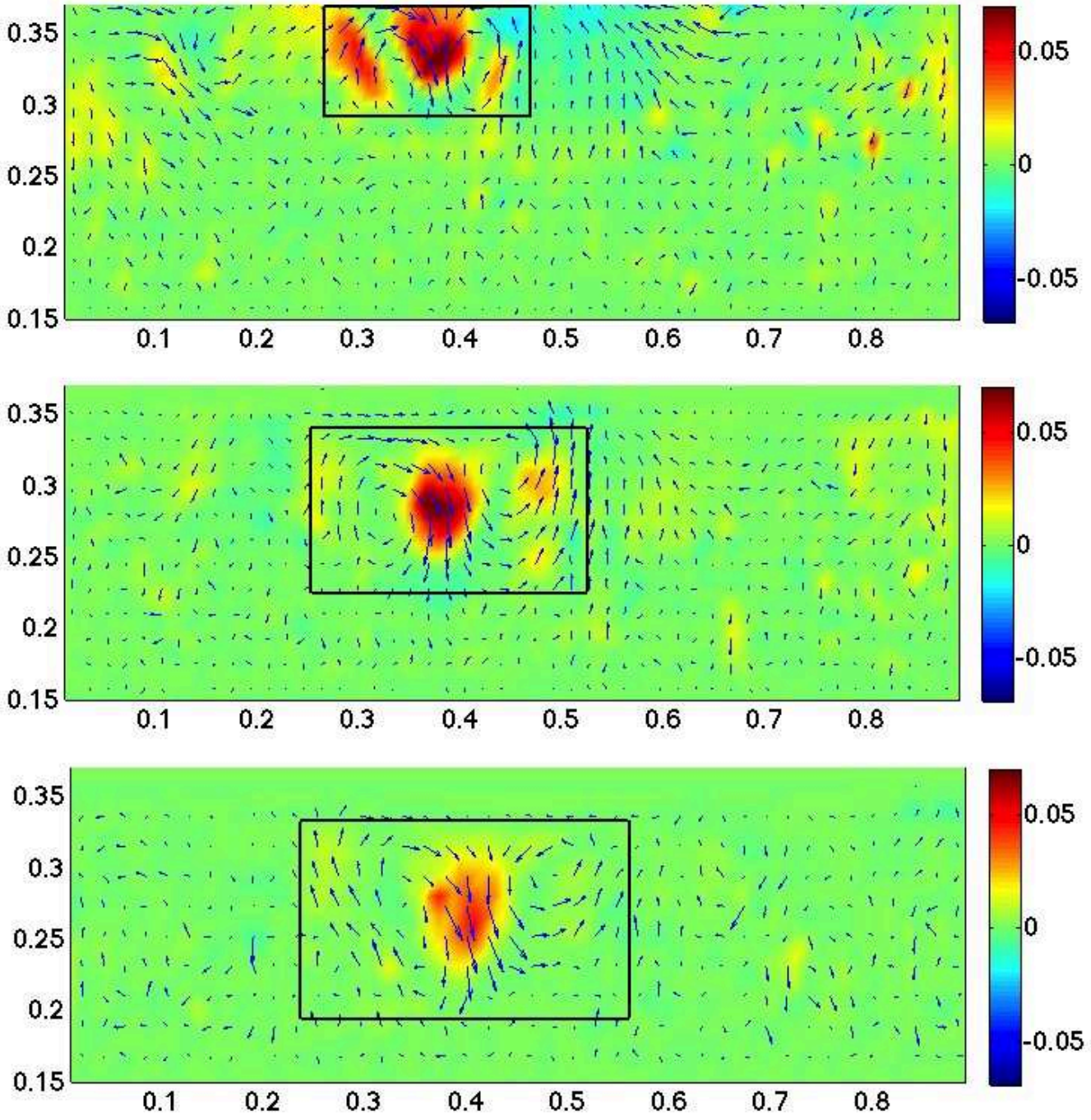

Fig. 7. Turbulent momentum flux ($-u'w'$) and turbulent velocity vectors (v', w') at time = 4.7, 5.1, 5.5 s

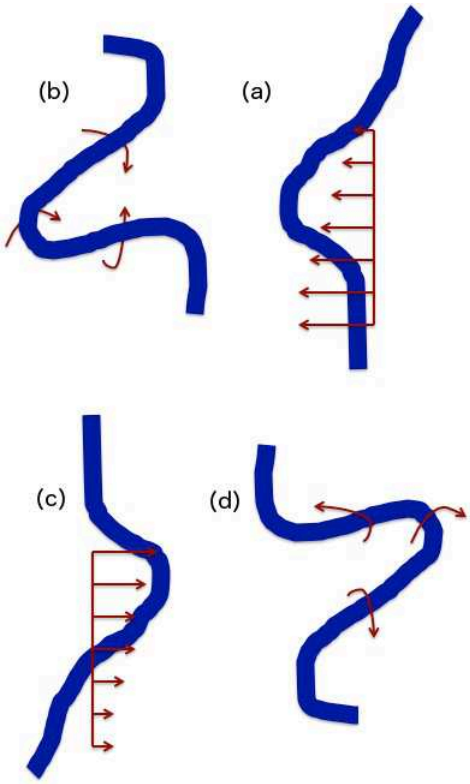

Fig. 5. Schematic illustration of a horseshoe (hairpin) vortex evolution in a turbulent flow. Top: Wave breaking problem in a wave-following frame of reference (reversed horseshoe structure), Bottom: Boundary layer problem (horseshoe structure) (a): vertical velocity profile in a wave-following frame of reference of a wave breaking problem and the generation of a reversed horseshoe structure (b): a reversed horseshoe structure in a wave breaking problem (c): vertical velocity profile in a boundary layer problem and the generation of a horseshoe structure (d): a horseshoe structure in a boundary layer problem

in this case. The horizontal rollers that are generated under the broken wave hit the bottom by the plunging breaker and no reversed horseshoe structure is generated. The numerical results are consistent with the experimental results of Ting and Kirby (1994, 1995, 1996).

IV. Conclusion

The three-dimensional GPUSPH numerical is used to model the generation, propagation, and breaking of a spilling solitary wave and a plunging solitary wave. SPH method is capable of modeling the broken solitary wave as well as the turbulent vortices generated under a broken wave. Two types of coherent vortex structures are observed under a broken wave: First is the spanwise two-dimensional rollers that are generated at the locations where the wave overturns and hits the surface ahead; Second is the three-dimensional reversed horseshoe structures that are initiated from the spanwise rollers and have a obliquely descending motion. These reversed horseshoe structures carry turbulent kinetic energy and momentum flux downward and can have a crucial role in the sediment transportation. Two legs of the reversed horseshoe structures have a counter-rotating rotations and high values of turbulent kinetic energy and Reynolds stresses were observed at the regions between the two counter-rotating legs and at the outer corner of them.

References

[1] M. L. Banner and D. H. Peregrine, *Wave Breaking in deep water*, Annual Review of Fluid Mechanics, 25, 373-379, 1993.
[2] E. D. Christensen, and R. Deigaard, *Large eddy simulation of breaking waves*, Coastal Engineering, 42, 53-86, 2001.
[3] A. Colagrossi, and M. Landrini, , *Numerical simulation of interfacial flows by smoothed particle hydrodynamics*, Journal of Computational Physics, 191, 448-475, 2003.
[4] R. A. Dalrymple, O. Knio, D. T. Cox, M. Gómez-Gesteira, and S. Zou, *Using a Lagrangian particle method for deck overtopping*, Proc. of Waves, ASCE., 1082-1091, 2002.
[5] R. A. Dalrymple and B. D. Rogers, *Numerical modeling of water waves with SPH method*, Coastal Engineering, 53, 141-147, 2006.
[6] R. J. Farahani, R. A. Dalrymple, A. Hérault, G. Bilotta,*Three-Dimensional SPH Modeling of a Bar/Rip Channel System*, Journal of Waterway, Port, Coastal, and Ocean Engineering, 140, pp. 82-99, 2014a.
[7] R. J. Farahani, R. A. Dalrymple, *Three-dimensional reversed horseshoe vortex structures under broken solitary waves*, Coastal Engineering Journal, under revision.
[8] S. I. Green, *Fluid Vortices*, Kluwer Academic Publishers, 1995.
[9] D. Goring, F. Raichlen, *The generation of long waves in the laboratory*, Coastal Engineering, 763-783, 1980.
[10] A. Hérault, G. Bilotta, A. Vicari, E. Rustico, and C. D. Negro, *Numerical simulation of lava flow using a GPU SPH model*, Annals of Geophysics, 54(5), 600-620, 2011.
[11] A. K. M. Hussain, *Coherent structures and turbulence*, Journal of Fluid Mechanics, 173., 303-356, 1986.
[12] J. Jeong, and F. Hussain, *On the identification of a vortex*, Journal of Fluid Mechanics, 285, 69-94, 1994.
[13] J. Kim, and P. Moin, *The structure of the vorticity field in turbulent channel flow. Part 2. Study of ensemble-averaged fields*, Journal of Fluid Mechanics, 162, 339-363, 1986.
[14] J. J. Monaghan and A. Kos, *Solitary waves on a certain beach*, Journal of Waterway, Port, Coastal and Ocean Engineering, 145-154, 1999.
[15] J. J. Monaghan and A. Kos, *Scott Russells wave generator*, Physics of Fluids, 12(3), 622-630, 2000.
[16] K. Nadaoka, M. Hino, and Y. Koyano, *Structure of the turbulent flow field under breaking waves in the surf zone*, Journal of Fluid Mechanics, 204, 359-387, 1989.
[17] F. C. K. Ting and J. T. Kirby, *Observation of undertow and turbulence in a laboratory surf zone*, Coastal Engineering, 24, 52-80,1994.
[18] F. C. K. Ting and J. T. Kirby, *Dynamics of surf zone turbulence in a strong plunging breaker*, Coastal Engineering, 24, 177-204, 1995.
[19] F. C. K. Ting and J. T. Kirby, *Dynamics of surf zone turbulence in a spilling breaker*, Coastal Engineering, 27, 131-160,1996.
[20] F. C. K. Ting *Large-scale turbulence under a solitary wave*, Coastal Engineering, 53, 441-462, 2006.
[21] Y. Watanabe and H. Saeki, *Three-dimensional large eddy simulation of breaking waves*, Coastal Engineering, 41, 281-301, 1999.
[22] H. Wendland, *Piecewise polynomial, positive definite and compactly supported radial functions of minimal degree*, Advances in Computational Mathematics, 4, 389-396, 1995.
[23] D. Yang, L. Shen, *Characteristics of coherent vortical structures in turbulent flows over progressive surface waves*, Physics of Fluids, 21, 125106, 1-23, 2009.

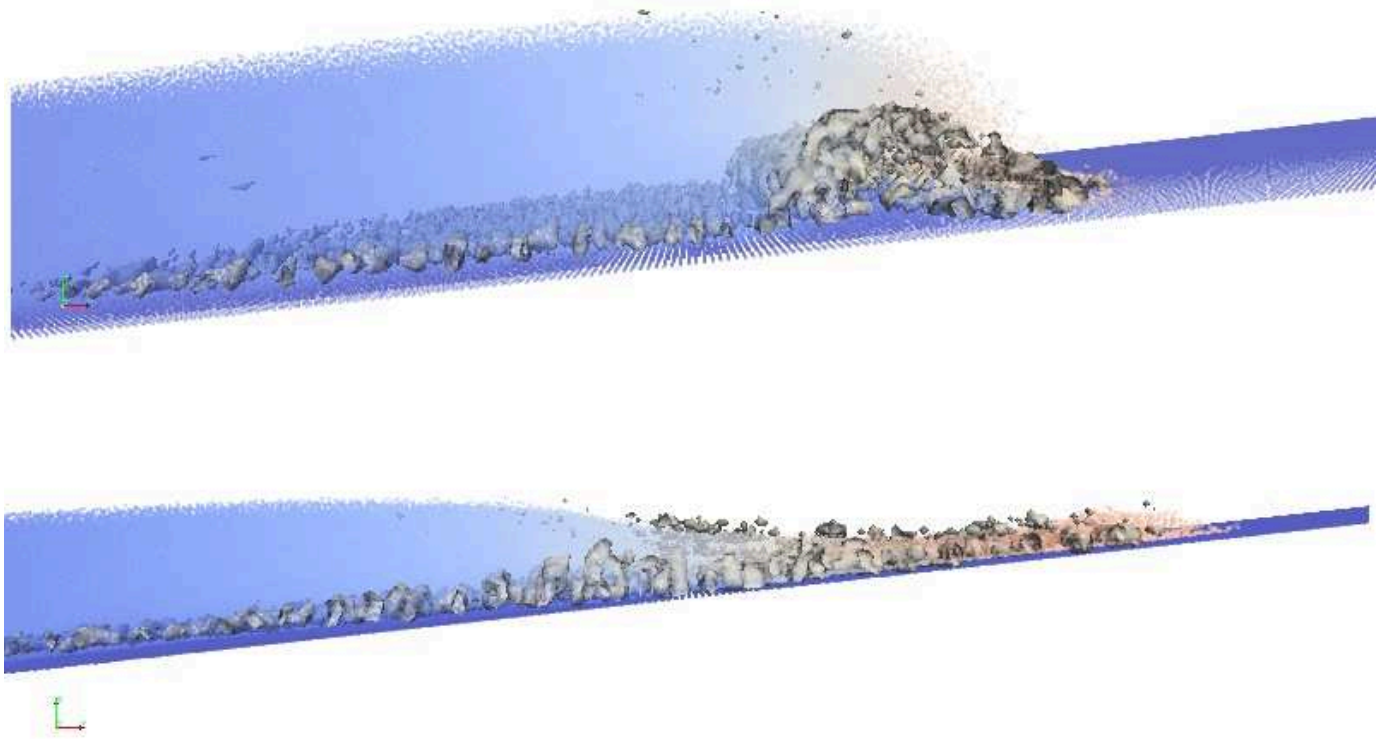

Fig. 8. Plunging solitary wave breaking and vortex structures detected by the isosurfaces of $\lambda_2 = -50$. Top: time = 3.1 s, Bottom: time = 3.3 s